Archimedean-based supramolecular cages ...

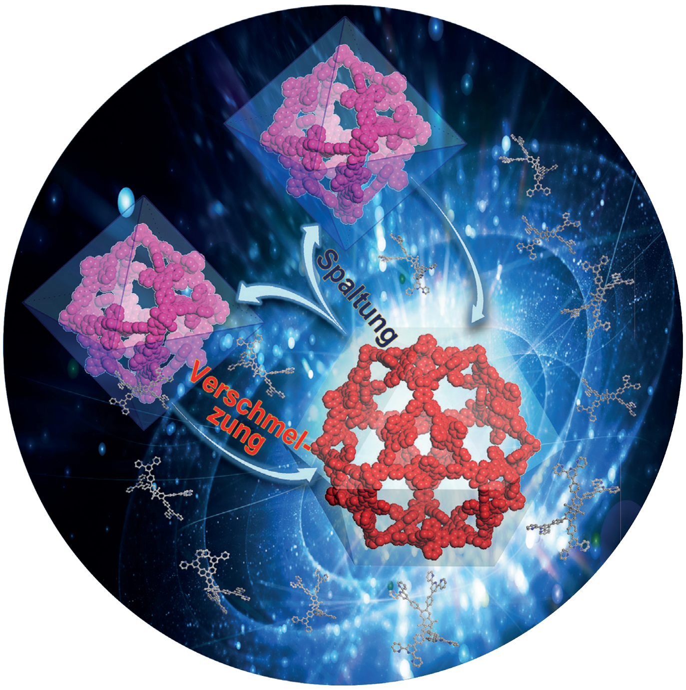

... are stoichiometrically synthesized from a bent, X-type, terpyridine-based ligand and Zn^{2+} or Cd^{2+} ions as described by G. R. Newkome, C. Wesdemiotis et al. in their Communication on page 9224 ff. Triggered by changing the concentration or the counterions, these unique materials undergo a fission–fusion process between a cuboctahedron and two octahedra that is reminiscent of the well-known biological processes observed in cell replication.

Intermetallic Phases

M. G. Kanatzidis and co-workers describe in their Communication on page 9186 ff. an intermetallic semiconductor that adopts a non-centrosymmetric structure. The band gap in $EuIr_4In_2Ge_4$ is a direct result of strong Ir–Ir bonding.

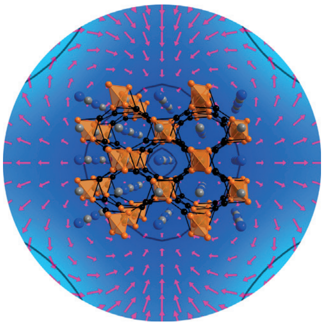

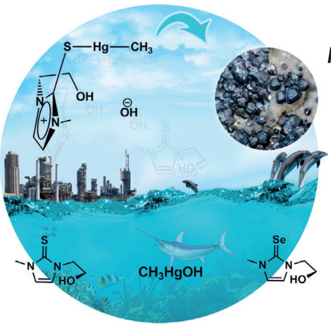

Mercury Pollutants

A method for the detoxification of organomercurials using *N*-methylimidazole-based thiones/selones under physiologically and environmentally relevant conditions is described by G. Roy and co-workers in their Communication on page 9323 ff.

High Oxidation States

In their Communication on page 9280 ff., M.-S. Miao et al. show by first-principles calculations that Hg can form stable compounds of HgF_4, a molecular crystal, and HgF_3, a metallic, ferromagnetic extended solid, under high pressure.

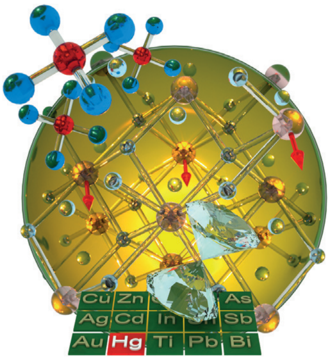

How to contact us:

Editorial Office:
E-mail: angewandte@wiley-vch.de
Fax: (+49) 6201–606-331
Telephone: (+49) 6201–606-315

Reprints, E-Prints, Posters, Calendars:
Carmen Leitner
E-mail: chem-reprints@wiley-vch.de
Fax: (+49) 6201–606-331
Telephone: (+49) 6201–606-327

Copyright Permission:
Bettina Loycke
E-mail: rights-and-licences@wiley-vch.de
Fax: (+49) 6201–606-332
Telephone: (+49) 6201–606-280

Online Open:
Margitta Schmitt
E-mail: angewandte@wiley-vch.de
Fax: (+49) 6201–606-331
Telephone: (+49) 6201–606-315

Subscriptions:
www.wileycustomerhelp.com
Fax: (+49) 6201–606-184
Telephone: 0800 1800536 (Germany only)
+44(0) 1865476721 (all other countries)

Advertising:
Marion Schulz
E-mail: mschulz@wiley-vch.de
Fax: (+49) 6201–606-550
Telephone: (+49) 6201–606-565

Courier Services:
Boschstrasse 12, 69469 Weinheim

Regular Mail:
Postfach 101161, 69451 Weinheim

Angewandte Chemie International Edition is a journal of the Gesellschaft Deutscher Chemiker (GDCh), the largest chemistry-related scientific society in continental Europe. Information on the various activities and services of the GDCh, for example, cheaper subscription to *Angewandte Chemie International Edition*, as well as applications for membership can be found at **www.gdch.de** or can be requested from GDCh, Postfach 900440, D-60444 Frankfurt am Main, Germany.

GDCh
GESELLSCHAFT
DEUTSCHER CHEMIKER

© 2015 Wiley-VCH Verlag GmbH & Co. KGaA, Weinheim

Get the Angewandte App
International Edition

Available on the App Store

Enjoy Easy Browsing and a New Reading Experience on the iPad or iPhone
- Keep up to date with the latest articles in Early View.
- Download new weekly issues automatically when they are published.
- Read new or favorite articles anytime, anywhere.

Editorial

"... The European Commission decided to launch the Graphene Flagship Project in 2013. The project brings together leading research laboratories from all over Europe with a wide span of different expertise. The Graphene Flagship (together with the Human Brain Project) is the largest collaborative research project that has ever been set up in Europe ..."
Read more in the Editorial by Andreas Hirsch.

Service

Author Profile

"If I won the lottery, I would open an art gallery. My biggest motivation is to keep learning new things ..."
This and more about Marinella Mazzanti can be found on page 9154.

© 2015 Wiley-VCH Verlag GmbH & Co. KGaA, Weinheim

News


M. C. Y. Chang


D. C. Crans


A. M. Echavarren


B. L. Feringa


M. A. Garcia-Garibay


N. K. Garg

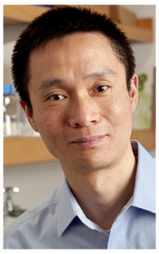
C. He


K. Itami


K. M. Nicholas


R. Sarpong

Highlights

Universal Blood

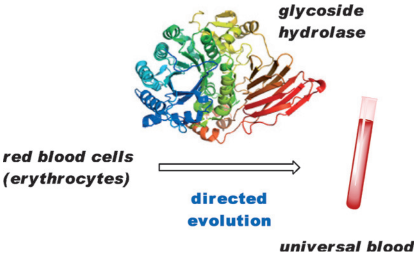

Coming closer to a vision: Directed evolution has been applied to a glycoside hydrolase for increased activity in the selective cleavage of A- and B-antigens from linkages on red blood cell surface glycans. The results are a major step forward in the challenging endeavor of producing universal blood.

Reviews

Biomolecular NMR Spectroscopy

A new spin on bio-NMR: This Review presents a state-of-the-art description of the leading approaches being considered today to improve the sensitivity of NMR spectroscopy, particularly as applied in biomolecular settings. The focus is on the future of ultrahigh-field NMR systems, emerging NMR detection technologies, new approaches to nuclear hyperpolarization, and progress in sample preparation.

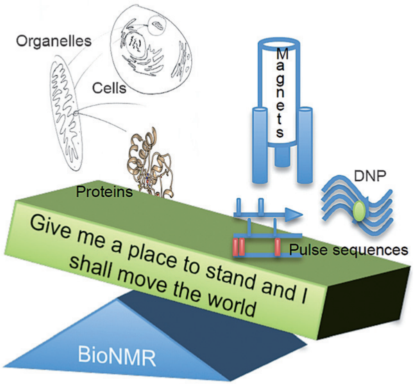

For the USA and Canada:
ANGEWANDTE CHEMIE International Edition (ISSN 1433-7851) is published weekly by Wiley-VCH, PO Box 191161, 69451 Weinheim, Germany. US mailing agent: SPP, PO Box 437, Emigsville, PA 17318. Periodicals postage paid at Emigsville, PA. US POSTMASTER: send address changes to *Angewandte Chemie*, John Wiley & Sons Inc., C/O The Sheridan Press, PO Box 465, Hanover, PA 17331. Annual subscription price for institutions: US$ 11.738/10.206 (valid for print and electronic / print or electronic delivery); for individuals who are personal members of a national chemical society prices are available on request. Postage and handling charges included. All prices are subject to local VAT/sales tax.

© 2015 Wiley-VCH Verlag GmbH & Co. KGaA, Weinheim

An intermetallic semiconductor with a non-centrosymmetric structure and the chemical formula $EuIr_4In_2Ge_4$ is reported. The band gap is a direct result of strong Ir–Ir bonding, and strong spin–orbit coupling effects lead to spin splitting at the conduction- and valence-band edges, which is described by the Dresselhaus term.

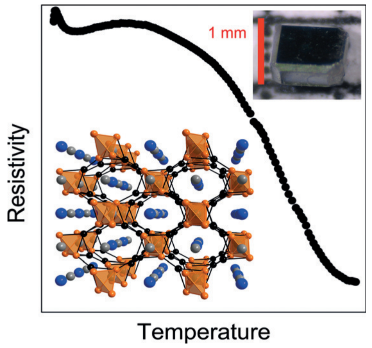

Frontispiece

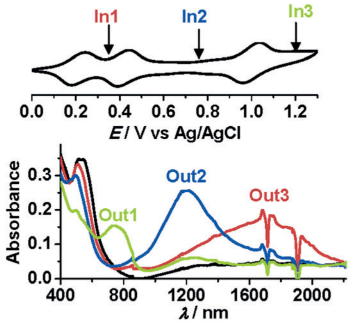

A diruthenium complex with a redox-active amine bridge shows three well-separated redox processes with exclusive near-infrared (NIR) absorbance at each redox state. The flip-flop, flip-flap-flop, and ternary memory have been realized by using the electropolymerized film (15–20 nm thick) of a related vinyl-functionalized complex with three electrochemical inputs and three NIR optical outputs.

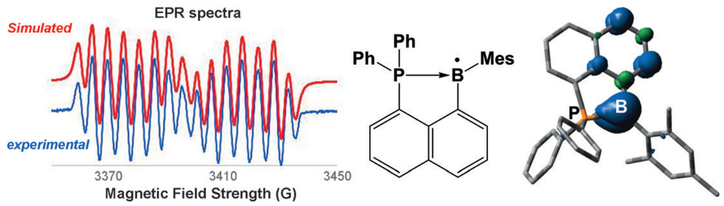

Radical action: A P-coordinated boryl radical with large spin density at the boron center is reported. The structure of the radical has been analyzed by EPR spectroscopy and using DFT calculations. The radical is found to undergo dimerization by a Gomberg-type dimerization process.

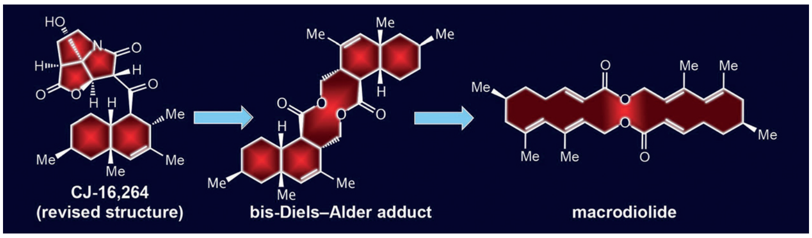

CJ-16,264 demystified: A pursuit of the originally assigned structure of antibiotic CJ-16,264 through a novel strategy featuring a double transannular Diels–Alder reaction led to its first total synthesis and structural revision.

© 2015 Wiley-VCH Verlag GmbH & Co. KGaA, Weinheim

Synthetic Methods

T. V. Q. Nguyen, W.-J. Yoo,
S. Kobayashi* ———— **9209 – 9212**

Effective Formylation of Amines with Carbon Dioxide and Diphenylsilane Catalyzed by Chelating bis(*tz*NHC) Rhodium Complexes

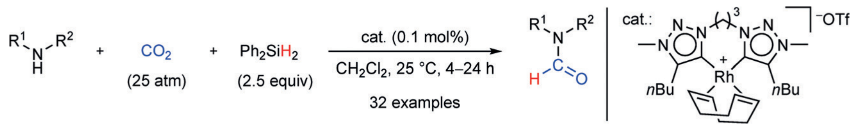

Beyond the norm: Rhodium complexes bearing a strong electron-donating bis(1,2,3-triazol-5-ylidene) ligand were found to be excellent catalysts for the reductive formylation of amines with CO_2 and Ph_2SiH_2 at ambient temperature. The catalyst system possesses a broad substrate scope which tolerates a variety of reducible functional groups and is suitable for the synthesis of bioactive compounds. Tf = trifuoromethanesulfonyl.

Molecular Recognition

T.-Y. Kuo, W.-H. Tseng,
C.-h. Chen* ———— **9213 – 9217**

Force Spectroscopy of Metal–Crown Ether Multivalency: Effect of Local Environments on Energy Landscape and Sensing Kinetics

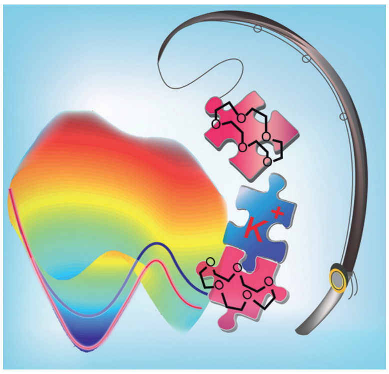

Break it up! The mechanical strength of metal–crown ether multivalent interactions is unveiled quantitatively by single-molecule force spectroscopy. The rupture force is on the order of tens of pico-Newton. Dynamic force spectroscopy shows that the effect of local environments is distinct on affinity association yet relatively insignificant on the dissociation reaction.

Nanomedicine

J. Wu, L. Zhao, X. Xu, N. Bertrand,
W. I. Choi, B. Yameen, J. Shi, V. Shah,
M. Mulvale, J. L. MacLean,
O. C. Farokhzad* ———— **9218 – 9223**

Hydrophobic Cysteine Poly(disulfide)-based Redox-Hypersensitive Nanoparticle Platform for Cancer Theranostics

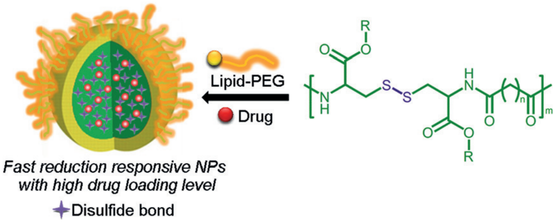

Fatty diacid monomers were used to develop a hydrophobic cysteine poly(disulfide)-based redox-sensitive nanoparticle platform for cancer theranostics. With this model system, the relationships between polymer structure, nanoparticle hydrophobicity, and redox responsibility were demonstrated. In vitro and in vivo results showed excellent anticancer performance.

Archimedean Polyhedra

T.-Z. Xie, K. Guo, Z. Guo, W.-Y. Gao,
L. Wojtas, G.-H. Ning, M. Huang, X. Lu,
J.-Y. Li, S.-Y. Liao, Y.-S. Chen,
C. N. Moorefield, M. J. Saunders,
S. Z. D. Cheng, C. Wesdemiotis,*
G. R. Newkome* ———— **9224 – 9229**

Precise Molecular Fission and Fusion: Quantitative Self-Assembly and Chemistry of a Metallo-Cuboctahedron

Bigger and bigger: A giant, 6 nm, shape-persistent, Archimedean-inspired cuboctahedron was quantitatively assembled and characterized by synchrotron X-ray analysis. The structure consists of one type of X-shaped, terpyridine-based ligand and 24 metal ions (Zn^{2+} or Cd^{2+}). A fusion–fission switching process between a cuboctahedron and an octahedron could be induced by changing the concentration or the counterions.

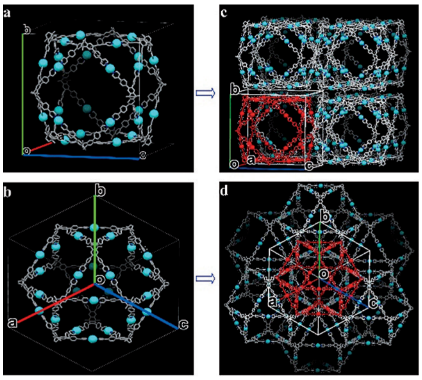

Front Cover

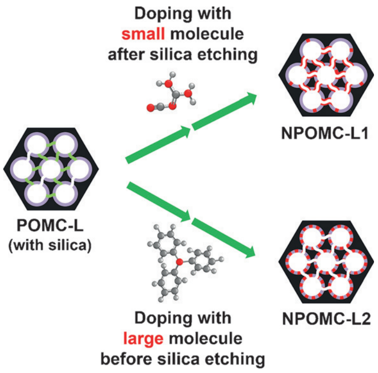

Controlling the pore size and doping site position of metal-free catalysts is the key to the synthesis of highly active metal-free catalysts for membrane electrode assemblies. Both have a critical influence on the accessibility of reactants to doping sites. A metal-free catalyst with a large pore size and precisely controlled doping site positions provides highly accessible doping sites, resulting in an outstanding single-cell performance.

Electrocatalysis

S. Lee, M. Choun, Y. Ye, J. Lee, Y. Mun,
E. Kang, J. Hwang, Y.-H. Lee, C.-H. Shin,
S.-H. Moon, S.-K. Kim, E. Lee,
J. Lee* **9230–9234**

Designing a Highly Active Metal-Free Oxygen Reduction Catalyst in Membrane Electrode Assemblies for Alkaline Fuel Cells: Effects of Pore Size and Doping-Site Position

Like a NP-needle in an azide-stack: Metal oxide nanoparticles functionalized with alkyne- and azide-bearing phosphonic acids were assembled in defined stacks with precise control over region-selectivity and layer composition by the Huisgen 1,3-dipolar cycloaddition. Incorporation of these stacks into capacitor devices shows the general applicability of our process for the fabrication of electronic devices.

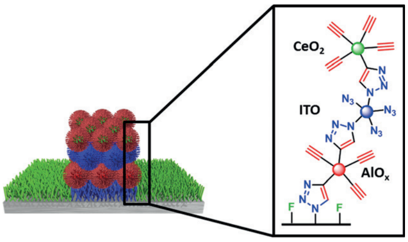

1,3-Dipolar Cycloaddition

S. H. Etschel, L. Portilla, J. Kirschner,
M. Drost, F. Tu, H. Marbach,
R. R. Tykwinski,* M. Halik* **9235–9238**

Region-Selective Deposition of Core–Shell Nanoparticles for 3 D Hierarchical Assemblies by the Huisgen 1,3-Dipolar Cycloaddition

A fast and viable route to isolated nanosheets is presented that is based on exfoliation studies on the protonated layered titanate $H_{1.07}Ti_{1.73}O_4{\cdot}H_2O$ (HTO). Direct exfoliation of HTO occurs within seconds after mixing of the reactants, instead via a swollen state as previously thought. This route is promising for large-scale synthesis of exfoliated nanosheets.

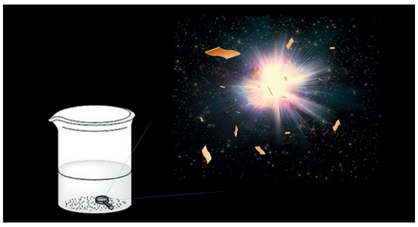

Nanosheets

H. Yuan, D. Dubbink, R. Besselink,
J. E. ten Elshof* **9239–9243**

The Rapid Exfoliation and Subsequent Restacking of Layered Titanates Driven by an Acid–Base Reaction

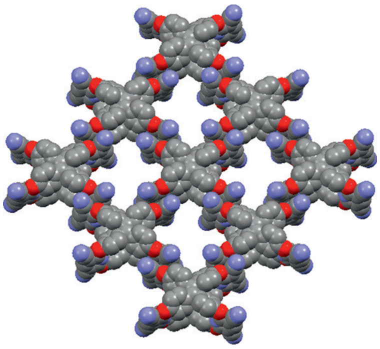

Emissive porous cage: A tricyclooxacalixarene cage molecule based on triphenylethylene (TPE) was prepared. The porous internal structure of the system gave rise to a good CO_2 uptake capacity and it showed a high selectivity for CO_2 adsorption over N_2. The cage molecule exhibited TPE fluorescence in solution and was used as a single-molecule platform to investigate the mechanism of aggregation-induced emission in TPE. Atom colors: C = gray; N = blue; O = red.

Cage Compounds

C. Zhang,* Z. Wang, L. Tan, T.-L. Zhai,
S. Wang,* B. Tan,* Y.-S. Zheng,*
X.-L. Yang, H.-B. Xu **9244–9248**

A Porous Tricyclooxacalixarene Cage Based on Tetraphenylethylene

© 2015 Wiley-VCH Verlag GmbH & Co. KGaA, Weinheim

Thiol-Induced Etching

T. A. Dreier, C. J. Ackerson* **9249 – 9252**

Radicals Are Required for Thiol Etching of Gold Particles

A radical new insight: The final step in the synthesis of atomically defined gold clusters has remained mechanistically obscure. A thiol-induced etching step is proposed that is initiated by the oxygen diradical.

Aluminum Hydroxides

D. Reusser, W. H. Casey,
A. Navrotsky* **9253 – 9256**

Energetic Insight into the Formation of Solids from Aluminum Polyoxocations

Inside Cover

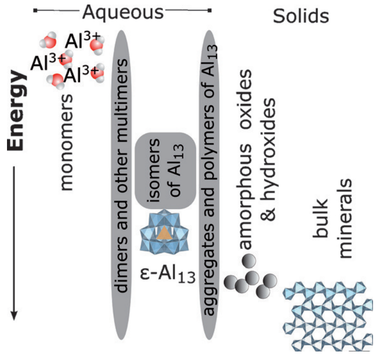

Downhill: Calorimetric measurements on the ε-$AlAl_{12}^{7+}$ ion and its heterometal-substituted forms provide the first enthalpy of formation ($\Delta H^{\circ}_{f,el}$) values on these species in aqueous form independent of formation pathway. Data reveal the $AlAl_{12}^{7+}$ ion lies closer in energy to solid aluminum (oxy)hydroxide phases than aqueous monomers, thus explaining its role as a precursor to amorphous aluminum hydroxides (flocs).

Colloidal Crystals

M. Chen, Y. Zhang, S. Jia, L. Zhou,
Y. Guan, Y. Zhang* **9257 – 9261**

Photonic Crystals with a Reversibly Inducible and Erasable Defect State Using External Stimuli

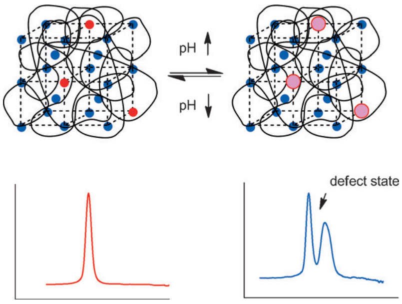

Artificial defects: Doped microgel colloidal crystals were facilely assembled from two microgels with the same size. A defect state in the crystals could be reversibly induced and erased by external stimuli (see picture).

Brønsted Superbases

I. Leito,* I. A. Koppel,* I. Koppel,
K. Kaupmees, S. Tshepelevitsh,
J. Saame **9262 – 9265**

Basicity Limits of Neutral Organic Superbases

Touching the limits: The possible limits of superbasicity achievable with families of neutral bases by expanding the molecular framework are explored. A simple model connecting basicity to the extent of the framework is proposed, validated, and used for quantitative predictions. Some of the considered compound families are expected to reach a gas-phase basicity of 340–370 kcal mol^{-1}, thus being among the most basic ever reported.

© 2015 Wiley-VCH Verlag GmbH & Co. KGaA, Weinheim

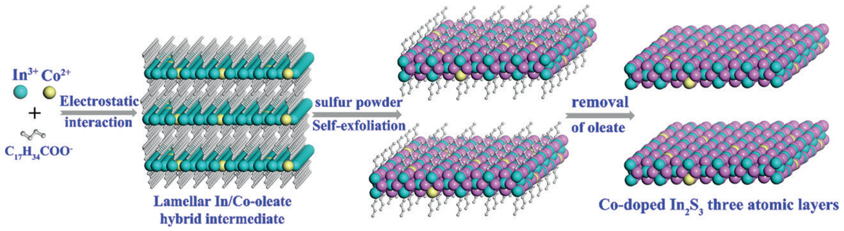

Cobalt doping confined in three atomic layers of In_2S_3 is implemented by a lamellar hybrid intermediate strategy. Ultrafast transient absorption spectroscopy shows that the ultrashort electron transfer time (ca. 1.6 ps) from the valence band to newly formed localized states is due to Co doping.

Doped Materials

A solar-driven chargeable Li-S battery has been developed by introducing a Pt/CdS photocatalyst in the aqueous polysulfide cathode. The most remarkable feature of this designed device is the simultaneous realization of both large-scale electrochemical storage and chemical fuel conversion of solar energy in one device, thus opening a new research area in pursuit of renewable clean energy.

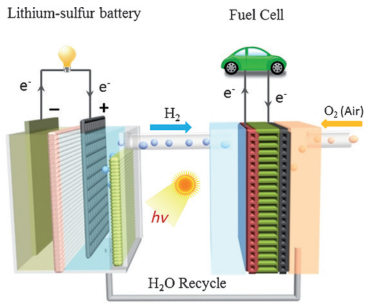

Photoenergy Storage

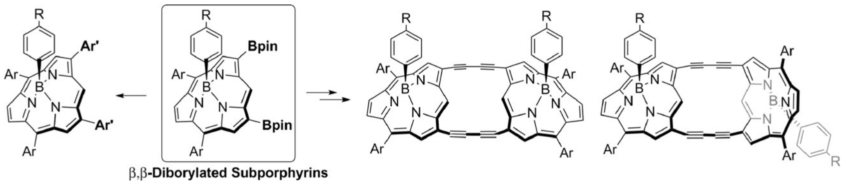

Iridium-catalyzed borylation of *B*-aryl *meso*-free subporphyrinato boron(III) complexes with bis(pinacolato)diboron effectively produced 2,13-diborylated subporphyrins regioselectively in good yields. These borylated species serve as promising synthetic precursors for 2,13-diarylated subporphyrins and doubly β-to-β 1,3-butadiyne-bridged subporphyrin dimers.

Porphyrinoids

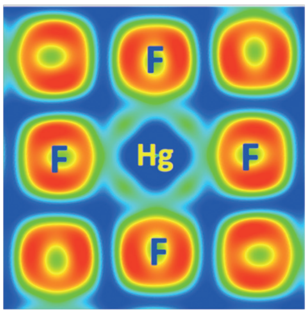

Mercury rising: Thermodynamically stable forms of crystalline HgF_3 and HgF_4 have been identified by ab initio calculations using DFT and PSO structure search methods. The Hg is in a high oxidation state and its 5d electrons are involved in forming chemical bonds. HgF_4 is a molecular crystal consisting of square-planar HgF_4 molecules. HgF_3 is an extended solid and exhibits exotic properties. It is metallic, ferromagnetic, and transparent to visible light.

Theoretical Chemistry

Back Cover

© 2015 Wiley-VCH Verlag GmbH & Co. KGaA, Weinheim

Metal–Organic Frameworks

T. H. Noh, H. Lee, J. Jang,
O.-S. Jung* ______ 9284–9288

Organization and Energy Transfer of Fused Aromatic Hydrocarbon Guests within Anion-Confining Nanochannel MOFs

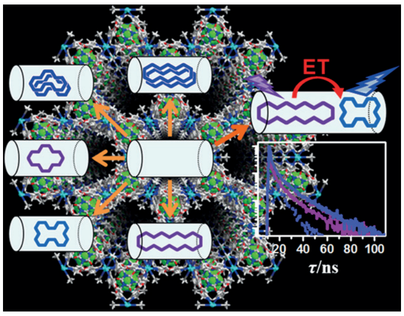

Slotted into place: The direct inclusion and organization of fused aromatic hydrocarbons (FAHs) within the hydrophobic 1D nanochannels of 3D metal–organic frameworks (MOFs) $[Zn_3L_4(CH_3CN)_6](X)_6$ (L = 1,3,5-tris(isonicotinoyloxyethyl)cyanurate; $X^- = BF_4^-$ and ClO_4^-) is reported. Förster resonance energy transfer (FRET) with the nanochannels from one FAH derivative to another is described.

Biocatalysis

M. E. Dirks-Hofmeister, T. Verhaeghe,
K. De Winter, T. Desmet* ______ 9289–9292

Creating Space for Large Acceptors: Rational Biocatalyst Design for Resveratrol Glycosylation in an Aqueous System

Biocatalyst design: Based on modeling and docking studies, a thermostable sucrose phosphorylase was engineered to enable access of large acceptor substrates. The site-specific loop variant R134A showed high transglycosylation activity on resveratrol in an aqueous system, requiring only sucrose as a cheap glycosyl donor. Significant promiscuity towards a range of other polyphenolic acceptors is also reported.

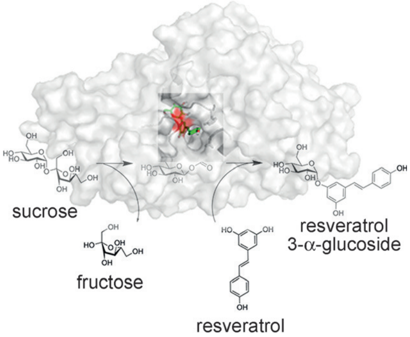

Synthetic Methods

H. Kondo, N. Akiba, T. Kochi,
F. Kakiuchi* ______ 9293–9297

Ruthenium-Catalyzed Monoalkenylation of Aromatic Ketones by Cleavage of Carbon–Heteroatom Bonds with Unconventional Chemoselectivity

Smaller is better: The title reaction for *ortho* C–O and C–N bonds of aromatic ketones was achieved. Direct comparison of the cleavage of the carbon–heteroatom bonds suggested an unconventional chemoselectivity, where smaller, more-electron-donating groups are more easily cleaved. Selective monofunctionalization of C–O bonds in the presence of *ortho* C–H bonds was also achieved.

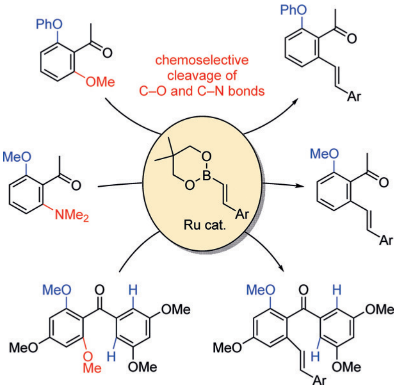

DNA Repair

S. Mondal, D. Manna,
G. Mugesh* ______ 9298–9302

Selenium-Mediated Dehalogenation of Halogenated Nucleosides and its Relevance to the DNA Repair Pathway

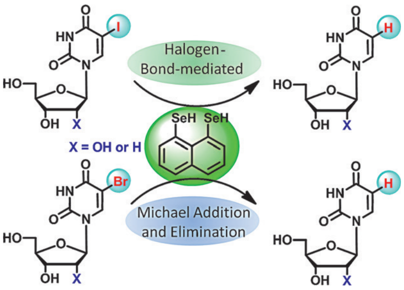

Saying goodbye to I: Selenium compounds are employed to mediate the dehalogenation of halogenated nucleobases and nucleosides in aqueous media under physiological conditions. These results may be important for the development of novel reagents for DNA modification and repair and suggest that Se derivatives may play a broader role in the metabolism of halogenated organic compounds in biology.

© 2015 Wiley-VCH Verlag GmbH & Co. KGaA, Weinheim

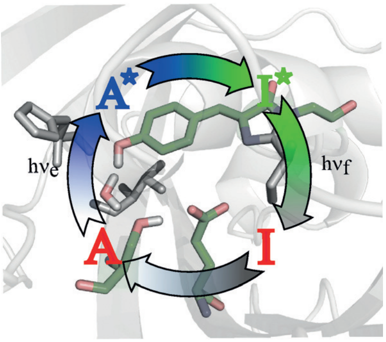

Protein proton wires: Light-activated proton transport in green fluorescent protein (GFP), which acts as a model for protein proton wires, has been characterized by femto- to microsecond time domain IR spectroscopy and mutagenesis studies. The results provide a detailed picture of the dynamics of long-range proton transfer in a protein.

Proton Transfer

S. P. Laptenok, A. Lukacs, A. Gil, R. Brust, I. V. Sazanovich, G. M. Greetham, P. J. Tonge,* S. R. Meech* **9303 – 9307**

Complete Proton Transfer Cycle in GFP and Its T203V and S205V Mutants

---

Throw a curve: An efficient route for the synthesis of electron-deficient tetrabenzo-fused pyracylenes (TBPs) is reported. TBP was found to undergo unique addition reactions with *n*-butyllithium and benzyne to give fluorescent compounds with a curved and planar π-system, respectively. These compounds showed distinct emission colors in the solid state with high quantum yields.

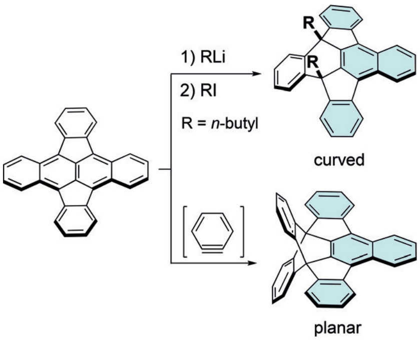

Fused-Ring Systems

Chaolumen, M. Murata,* Y. Sugano, A. Wakamiya, Y. Murata* **9308 – 9312**

Electron-Deficient Tetrabenzo-Fused Pyracylene and Conversions into Curved and Planar π-Systems Having Distinct Emission Behaviors

---

A microfluidic chip was developed taking advantage of a carbon fiber nanoelectrode (CFNE) and a robust platform for real-time monitoring of single intra-synaptic vesicular release events and of the subsequent generation of postsynaptic membrane excitatory potential (EJP) signals. By using this chip, the first in situ measurements of synaptic transmission in neuromuscular mimics are reported.

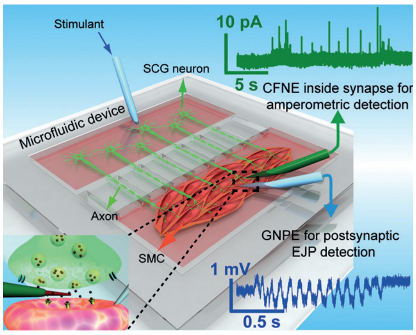

Nanobioanalysis

Y. T. Li, S. H. Zhang, X. Y. Wang, X. W. Zhang, A. I. Oleinick, I. Svir, C. Amatore,* W. H. Huang* **9313 – 9318**

Real-time Monitoring of Discrete Synaptic Release Events and Excitatory Potentials within Self-reconstructed Neuromuscular Junctions

---

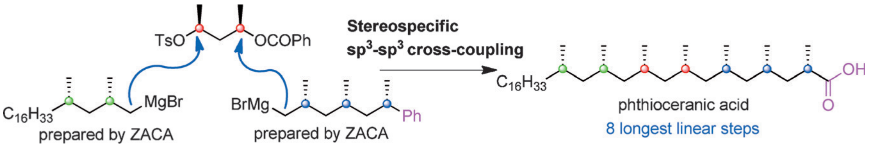

A step-economical synthesis of phthioceranic acid was achieved by using a conceptually new strategy. ZACA-Pd-catalyzed vinylation was used to prepare smaller deoxypropionate building blocks. Then two Cu-catalyzed stereospecific sp^3–sp^3 cross-couplings linked the smaller fragments together with full inversion of configuration to assemble large polydeoxypropionates in a stereoselective manner. ZACA = Zr-catalyzed asymmetric carboalumination of alkenes.

Natural Product Synthesis

S. Xu, A. Oda, T. Bobinski, H. Li, Y. Matsueda, E. Negishi* **9319 – 9322**

Highly Efficient, Convergent, and Enantioselective Synthesis of Phthioceranic Acid

© 2015 Wiley-VCH Verlag GmbH & Co. KGaA, Weinheim

Mercury Pollutants

M. Banerjee, R. Karri, K. S. Rawat,
K. Muthuvel, B. Pathak,
G. Roy* ________ **9323 – 9327**

Chemical Detoxification of Organomercurials

Inside Back Cover

Getting rid of mercury: Insoluble HgE (E = S, Se) nanoparticles (NPs) are formed under physiologically relevant conditions when organomercurials are treated with *N*-methylimidazole-based thiones/selones having an *N*-CH_2CH_2OH substituent. Compounds lacking the *N*-CH_2CH_2OH substituent failed to produce HgE NPs upon treatment with organomercurials under identical reaction conditions. A novel pathway of detoxifying various organomercurials is described.

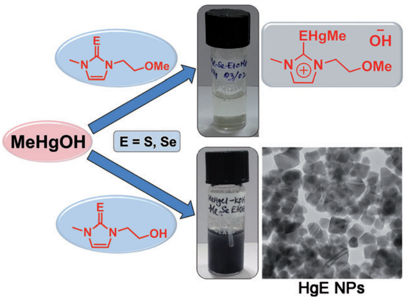

Borohydride Hydrolysis

L. Lu, H. Zhang,* S. Zhang,*
F. Li ________ **9328 – 9332**

A Family of High-Efficiency Hydrogen-Generation Catalysts Based on Ammonium Species

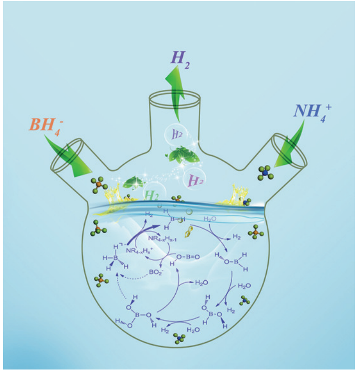

The catalytic activities of inorganic ammonium ions for hydrogen generation by the hydrolysis of borohydrides and the corresponding mechanisms were investigated. The catalytic activities were higher than or comparable to those of typical noble-metal/transition-metal catalysts but the ammonium ions are considerably cheaper, more environmentally friendly, and more readily available.

Chiral Polymer Catalysts

Y.-Z. Ke, Y. Nagata, T. Yamada,
M. Suginome* ________ **9333 – 9337**

Majority-Rules-Type Helical Poly(quinoxaline-2,3-diyl)s as Highly Efficient Chirality-Amplification Systems for Asymmetric Catalysis

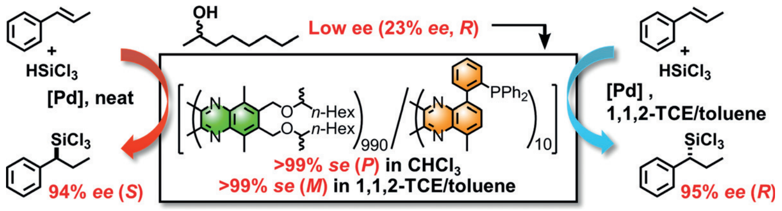

Bowing to the majority: Poly(quinoxaline-2,3-diyl) containing PPh_2 groups and chiral side chains derived from (*R*)-2-octanol with 23% *ee* exhibited a single-handed-helical conformation and served as a highly enantioselective chiral ligand in palladium-catalyzed reactions (see scheme; *se* = screw-sense excess). The chirality of the polymer could be switched by a solvent effect to enable the synthesis of the enantiomeric products.

Reactive Intermediates

S. Chatterjee, T. K. Paine* ________ **9338 – 9342**

Olefin *cis*-Dihydroxylation and Aliphatic C–H Bond Oxygenation by a Dioxygen-Derived Electrophilic Iron–Oxygen Oxidant

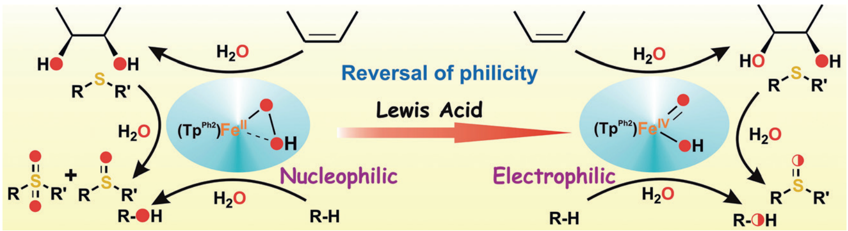

Lewis acid mediated O–O bond cleavage: A nucleophilic iron(II)–hydroperoxo oxidant, formed upon oxidative decarboxylation of an iron(II)–α-hydroxy acid complex, undergoes heterolytic O–O bond cleavage in the presence of a Lewis acid to generate an electrophilic iron(IV)–oxo–hydroxo oxidant. The electrophilic oxidant oxidizes sulfides to sulfoxides and alkenes to *cis*-diols, and it hydroxylates the strong C–H bonds of aliphatic substrates.

© 2015 Wiley-VCH Verlag GmbH & Co. KGaA, Weinheim

Bioconjugation

J. S. Lampkowski, J. K. Villa, T. S. Young, D. D. Young* ______ **9343 – 9346**

Development and Optimization of Glaser–Hay Bioconjugations

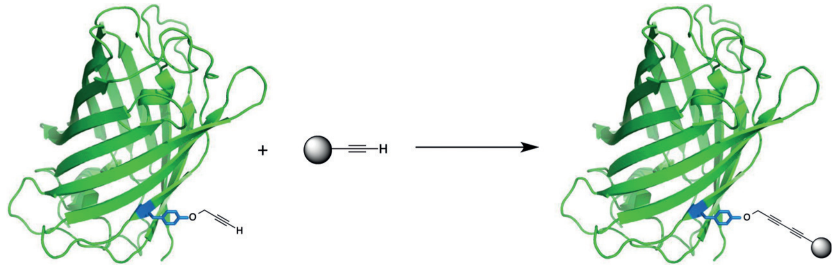

A Glaser–Hay bioconjugation has been developed. This new bioconjugation method affords well-defined, linear, highly oxidized bioconjugates. This is the first reported aqueous Glaser–Hay reaction and first utilization of this reaction in the conjugation of proteins, small molecules, and solid supports.

Synthetic Methods

T. Iwasaki,* R. Shimizu, R. Imanishi, H. Kuniyasu, N. Kambe* ______ **9347 – 9350**

Copper-Catalyzed Regioselective Hydroalkylation of 1,3-Dienes with Alkyl Fluorides and Grignard Reagents

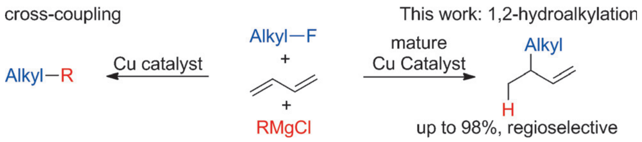

Making the switch: A copper–hydride species, generated by the treatment of a copper salt with alkyl Grignard reagents, catalyzes the 1,2-hydroalkylation of 1,3-dienes by alkyl fluorides and Grignard reagents. The alkyl group of the alkyl fluoride is selectively introduced to an internal carbon atom of the 1,3-diene and the Grignard reagent acts as hydride source to give the branched terminal alkene, even in the presence of alkenes and alkynes.

Water Splitting

C. Tang, N. Cheng, Z. Pu, W. Xing, X. Sun* ______ **9351 – 9355**

NiSe Nanowire Film Supported on Nickel Foam: An Efficient and Stable 3D Bifunctional Electrode for Full Water Splitting

NiSe nanowire films grown hydrothermally in situ on nickel foam (NiSe/NF) were used as a 3D bifunctional electrode for both the oxygen evolution reaction and hydrogen evolution reaction in a strongly alkaline electrolyte. The films exhibit high catalytic activity and superior stability, and a cell voltage of only 1.63 V is required for the alkaline water electrolyzer to deliver 10 mA cm^{-2} water-splitting current.

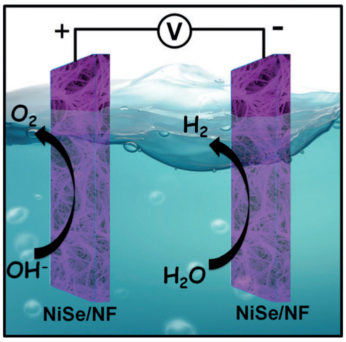

Synthetic Methods

F. Wang, N. Zhu, P. Chen, J. Ye, G. Liu* ______ **9356 – 9360**

Copper-Catalyzed Trifluoromethylazidation of Alkynes: Efficient Access to CF_3-Substituted Azirines and Aziridines

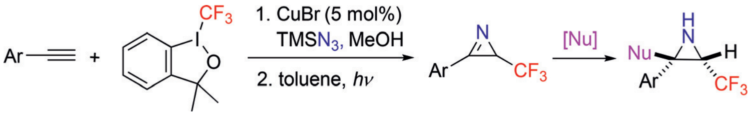

Az is: A novel method for convenient access to CF_3-containing azirines has been developed, and involves a copper-catalyzed trifluoromethylazidation of alkynes and a photocatalyzed rearrangement. Both terminal and internal alkynes are compatible with this reaction and deliver azirines in moderate to good yields. The azirines can be further converted into various CF_3-substituted aziridines. TMS = trimethylsilyl.

© 2015 Wiley-VCH Verlag GmbH & Co. KGaA, Weinheim

Porous Polymer Materials

P. F. Li, T. B. Schon,
D. S. Seferos* ____________ 9361 – 9366

Thiophene, Selenophene, and Tellurophene-based Three-Dimensional Organic Frameworks

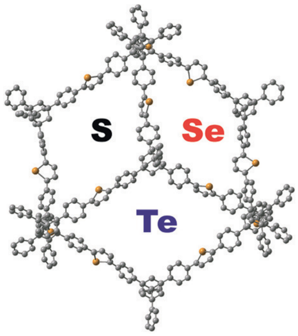

Elements control properties: 3D frameworks consisting of adamantane vertices and diphenylheterocycle (S, Se, and Te) linkers have been synthesized and characterized. The specific surface area and pore width of frameworks depends on the element incorporated in the heterocycle. Optoelectronic properties are also element dependent. A supercapacitor was constructed to demonstrate electronic activity.

Highly Energetic Compounds

H. Wei, C. He, J. Zhang,
J. M. Shreeve* ____________ 9367 – 9371

Combination of 1,2,4-Oxadiazole and 1,2,5-Oxadiazole Moieties for the Generation of High-Performance Energetic Materials

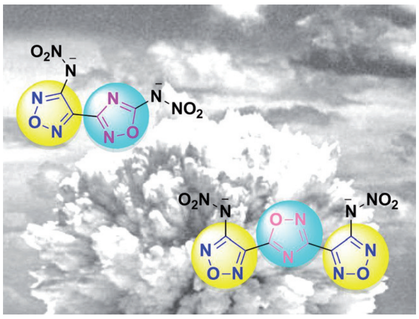

Bursting with energy: Two types of high-density energetic salts (see anion structures) were obtained by linking 1,2,4-oxadiazole and 1,2,5-oxadiazole precursors. The superior detonation performance and good thermal stability of the salts make them promising high-energy-density materials.

Pincer Complexes

K. J. Jonasson, A. V. Polukeev, R. Marcos,
M. S. G. Ahlquist,
O. F. Wendt* ____________ 9372 – 9375

Reversible α-Hydrogen and α-Alkyl Elimination in PC(sp^3)P Pincer Complexes of Iridium

An iridium pincer complex undergoes reversible α-alkyl elimination. Under certain conditions, this fundamentally new process for C(sp^3)–C(sp^3) bond cleavage has a low barrier that is comparable with that of well known α-hydrogen elimination reactions. Kinetic studies, activation parameters, and DFT calculations are also discussed.

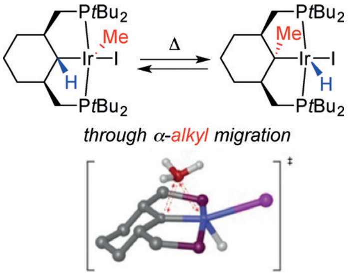

Supramolecular Chemistry

H.-L. Sun, Y. Chen, J. Zhao,
Y. Liu* ____________ 9376 – 9380

Photocontrolled Reversible Conversion of Nanotube and Nanoparticle Mediated by β-Cyclodextrin Dimers

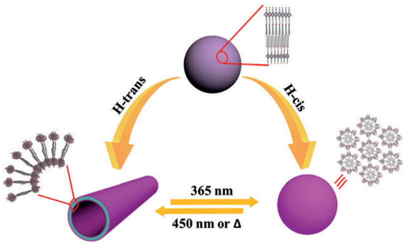

Photodriven interconversion: A photoswitchable supramolecular nanotube–nanoparticle system was constructed through secondary assembly of self-aggregates of amphiphilic porphyrin derivatives (see picture). These nanoassemblies repeatedly interconvert upon irradiation at 365 and 450 nm.

Stereoselective Deuteration

K. Moozeh, S. M. So,
J. Chin* ____________ 9381 – 9385

Catalytic Stereoinversion of L-Alanine to Deuterated D-Alanine

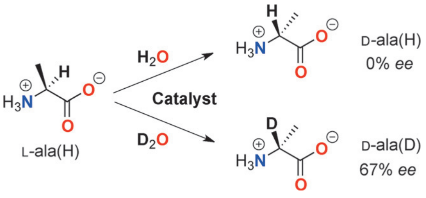

Deuteration of alanine with a combination of an achiral pyridoxal analogue and a chiral base as catalyst is stereoselective, but protonation is not. Thus a racemic mixture of alanine can be catalytically deuterated under mild conditions without the use of any protecting groups to give an enantiomeric excess of deuterated D-alanine.

© 2015 Wiley-VCH Verlag GmbH & Co. KGaA, Weinheim

Uranium Complexes

N. H. Anderson, H. Yin, J. J. Kiernicki,
P. E. Fanwick, E. J. Schelter,
S. C. Bart* ______ **9386 – 9389**

Investigation of Uranium Tris(imido) Complexes: Synthesis, Characterization, and Reduction Chemistry of $[U(NDIPP)_3(thf)_3]$

Reduced to dimers: $[U(NDIPP)_3(thf)_3]$ was isolated upon treatment of $[UI_3(thf)_4]$ with KC_8 in the presence of 2,6-diisopropylphenylazide (N_3DIPP). Crystallographic characterization shows an unprecedented *fac*-uranium tris(imido) species (see picture). Single-electron reduction of the complex formed the dimer $[K(Et_2O)]_2[U(NDIPP)_3]_2$, which was studied using variable-temperature/field magnetic measurements. Atom colors: U = pink; O = red; N = blue; C = black.

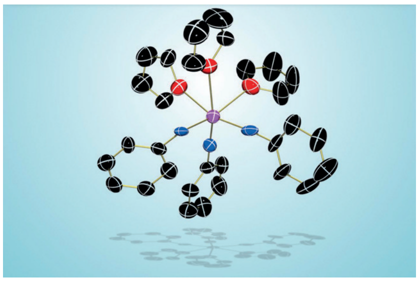

Organocatalysis

L. Zong, S. Du, K. F. Chin, C. Wang,
C.-H. Tan* ______ **9390 – 9393**

Enantioselective Synthesis of Quaternary Carbon Stereocenters: Addition of 3-Substituted Oxindoles to Vinyl Sulfone Catalyzed by Pentanidiums

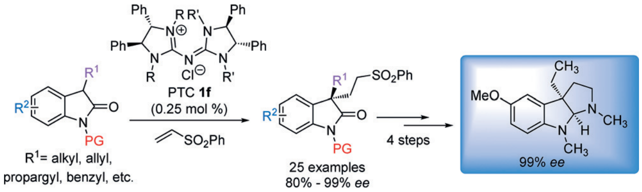

Efficiency of pentanidiums: Enantioselective conjugate addition between 3-alkyloxindoles and phenyl vinyl sulfone was achieved with a pentanidium phase-transfer catalyst. Various enantioenriched oxindole derivatives with versatile functional groups were synthesized. Gram-scale experiments also indicate the high efficiency and practicality of the current strategy.

Electrocatalysis

D.-J. Chen, Y. Y. J. Tong* ______ **9394 – 9398**

Irrelevance of Carbon Monoxide Poisoning in the Methanol Oxidation Reaction on a PtRu Electrocatalyst

The methanol oxidation reaction (MOR) on Ru/Pt thin film and commercial PtRu/C was studied by in situ attenuated total-reflection–surface-enhanced IR reflection absorption spectroscopy. A revised MOR enhancement mechanism is proposed in which CO on Pt sites is irrelevant but instead Pt–Ru boundary sites catalyze the oxygen insertion reaction that leads to the formation of bidentate formate (indicated as =OOCH) and enhances the direct reaction pathway.

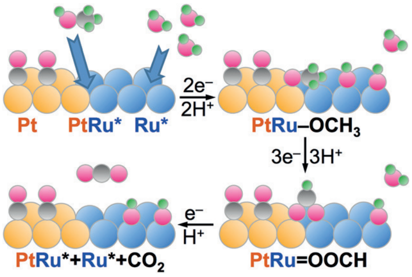

Biomass Conversion

J. L. Song,* B. W. Zhou, H. C. Zhou,
L. Q. Wu, Q. L. Meng, Z. M. Liu,
B. X. Han* ______ **9399 – 9403**

Porous Zirconium–Phytic Acid Hybrid: a Highly Efficient Catalyst for Meerwein–Ponndorf–Verley Reductions

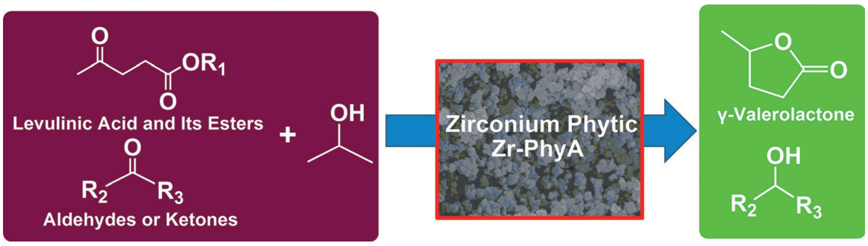

All natural: Porous zirconium phosphonate (Zr-PhyA) was synthesized simply by reaction of natural phytic acid (PhyA) and $ZrCl_4$ and applied as a very efficient catalyst for the Meerwein–Ponndorf–Verley reduction of various carbonyl compounds. Both the Zr element and phosphate groups contributed significantly to the excellent catalytic performance of Zr-PhyA.

© 2015 Wiley-VCH Verlag GmbH & Co. KGaA, Weinheim

C–H Activation

X. Huang, Y. Wang, J. Lan,
J. You* ——— **9404 – 9408**

Rhodium(III)-Catalyzed Activation of C_{sp^3}–H Bonds and Subsequent Intermolecular Amidation at Room Temperature

Giving direction: The title reaction leads to the successful functionalization of unreactive C_{sp^3}–H bonds in the presence of directing groups (DGs). A rhodacycle having a SbF_6^- counterion was isolated and is proposed to be a plausible intermediate.

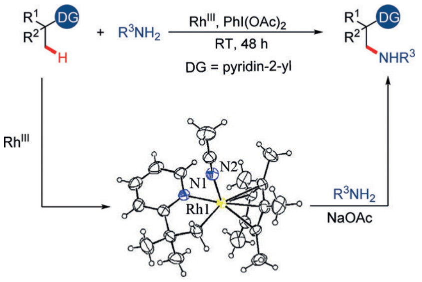

Organocatalysis

M.-Y. Wu, W.-W. He, X.-Y. Liu,*
B. Tan* ——— **9409 – 9413**

Asymmetric Construction of Spirooxindoles by Organocatalytic Multicomponent Reactions Using Diazooxindoles

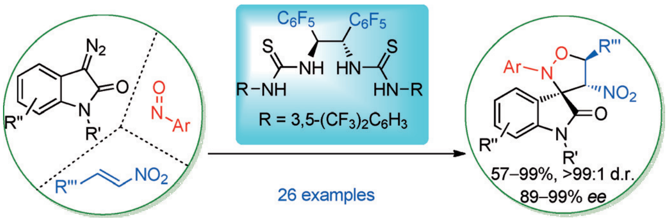

Multiple players: The first highly stereoselective multicomponent reaction of diazooxindoles, nitrosoarenes, and nitroalkenes with a newly developed hydrogen-bond catalyst has been successfully developed. The spirooxindole products are isolated in excellent yields and stereoselectivities, and contain three contiguous stereogenic centers. R''' = aryl or alkyl.

Synergistic Catalysis

S. Zhu,* Q. Zhang, K. Chen,
H. Jiang ——— **9414 – 9418**

Synergistic Catalysis: Metal/Proton-Catalyzed Cyclization of Alkynones Toward Bicyclo[3.*n*.1]alkanones

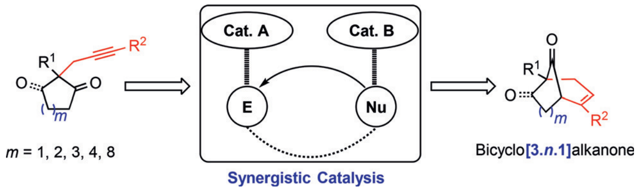

A highly efficient and practical synergistically metal/proton-catalyzed Conia–ene reaction for the synthesis of bicyclo[3.*n*.1]alkanones has been developed. The reaction was successfully utilized in modifying natural compounds such as methyl dihydrojasmonate, α,β-thujone, and 5α-cholestan-3-one. Furthermore, the bicyclo[3.2.1]alkanones can be ring-opened by nucleophiles to give the corresponding products in excellent yields.

Supporting information is available on www.angewandte.org (see article for access details).

A video clip is available as Supporting Information on www.angewandte.org (see article for access details).

This article is available online free of charge (Open Access).

This article is accompanied by a cover picture (front or back cover, and inside or outside).

The Very Important Papers, marked VIP, have been rated unanimously as very important by the referees.

The Hot Papers are articles that the Editors have chosen on the basis of the referee reports to be of particular importance for an intensely studied area of research.

© 2015 Wiley-VCH Verlag GmbH & Co. KGaA, Weinheim